Heterogeneous Multilink Aggregation for Reliable UAV Communication in Maritime Search and Rescue Missions

Johannes Güldenring, Lucas Koring, Philipp Gorczak and Christian Wietfeld
TU Dortmund University, Communication Networks Institute (CNI)
Otto-Hahn-Str. 6, 44227 Dortmund, Germany
{johannes.gueldenring, lucas.koring, philipp.gorczak, christian.wietfeld}@tu-dortmund.de

***Abstract*—Recent technological advances are leading to increasing adoption of Unmanned Aerial Vehicles (UAV) in more and more application areas. The use of UAVs promises great potentials in finding missing persons during maritime search and rescue (SAR) missions. Hereby, communication between ground station and vehicle is essential in order to exchange data. Mandatory requirements are high reliability - especially for telemetry and control data - as well as high data rates as an enabler for high resolution thermal imaging and real-time video payloads. The underlying paper investigates the applicability of Long Term Evolution (LTE) for maritime SAR missions. Therefore, in a first step, a detailed maritime channel model is developed and implemented. The analytic evaluations show significant decreases in communication range in dependency of UAV flight and base station height and in dependency of the current wind speed. To compensate interferences and frequency-dependent propagation effects the authors propose the aggregation of multiple LTE links using the Multipath TCP (MPTCP) protocol. The proposed multi-link concept is evaluated and assessed in a close-to-reality evaluation. Hereby, a hardware-in-the-loop (HIL) experiment is conducted emulating a public mobile network operator in combination with a dedicated SAR-mission-only LTE link. The experiments highlight the applicability of LTE and MPTCP for maritime SAR missions. The heterogeneous multilink concept increases UAV communication range and achieves high reliability and data rates in the whole search area.**

***Keywords*—Multipath TCP (MPTCP), Long-range Long Term Evolution (LTE), Unmanned Aerial Vehicle (UAV), Search and Rescure (SAR), Maritime Communication, Over-Sea.**

I. Introduction and Related Work

The fast-paced development of Unmanned Aerial Vehicle (UAV) widened their area of application in the past years [1]. One of these novel fields is addressed in the research project LARUS [2], where an UAV is utilized to support maritime search and rescue (SAR) missions. For a fast and accurate detection of missing people in large ocean territories, complex sensor techniques such as high-resolution camera systems or radio-based localization technology are necessary. To make use of the information gained by the UAV, data must be transferred to the Maritime Rescue Coordination Center (MRCC) on-flight and in real-time. Especially when considering additional control and telemetry data or further conceivable thermal imagery, the need for a reliable broadband communication system is obvious. As correctly depicted in [3] and [4], the mobile communication standard Long Term Evolution (LTE) as well as the uprising 5G technology are appropriate candidates for a robust and long-range UAV payload and control communication links in a maritime environment for SAR missions. Although the maritime rescue scenario is used as major reference, the technologies and research approaches presented in this contribution are relevant for robotics scenarios requiring reliable communication, for example terrestrial rescue robotics as well as logistics and industry.

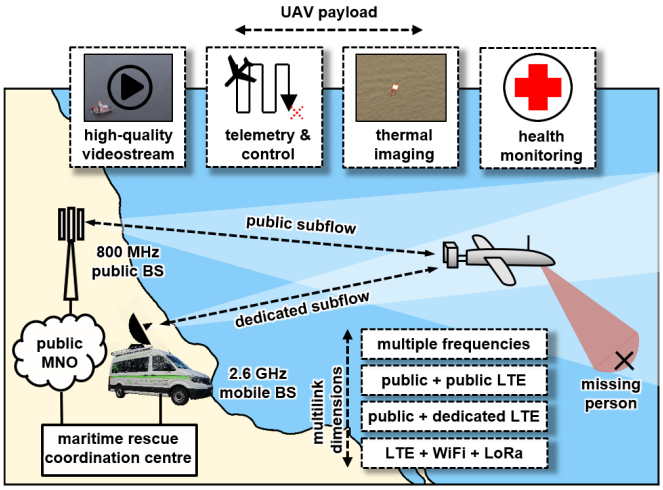

Fig. 1. Illustration of the proposed scenario and approach. An UAV is utilized as multiple sensor platform in order to support maritime search and rescue missions. The large amount of data generated must be transferred to the ground control station in a reliable and efficient way, for which a multilink concept is proposed.

The air-to-ground communication link of UAVs needs to be very reliable and constantly support high bandwidth. Therefore, this work proposes the concept of multi link aggregation to compensate insufficient network conditions, propagation effects and create redundancy. Fig. 1 illustrates the proposed approach. An UAV on a SAR mission is gathering information with a need for very high-bitrate and reliable Air-to-Ground (A2G) data transfer. Several approaches for multi-link aggregation exist. The most common approach, which is used within the scope of this paper, is Multipath TCP (MPTCP) [5]. MPTCP extends the fundamental Transmission Control Protocol (TCP) by establishing multiple, individual subflows for each network link. MPTCP achieves higher throughput and increased reliability as well as lower latency. Alternate

978-1-7281-3316-4/19/$31.00 ©2019 IEEE

approaches like *Multipath Quic* [6] and *Scalable Network Coding* [7] require significantly more resources, latter one especially in terms of computing power, due to their higher complexity and are therefore currently not implementable in lightweight UAV platforms. Energy efficient payload transport based on MPTCP for drones has been successfully evaluated in [8] and [9] even though experimental evaluation has not been conducted in maritime or SAR scenarios.

The applicability of LTE for over-sea missions has been evaluated in [10] and a coverage of up to 180 km was presented. To achieve this cell size, two base stations (BS) were used. The first BS served the UE in the distance of 0 km to 80 km, whereas the second BS range from 80 km to 180 km distance. Here, the high range of the second BS was achieved by the high radio front end placement at a coast-near mountain in the height of 1850 m and by leveraging strongly directed antennas. In addition, a modification of the LTE timing advance (TA) mechanism was proposed, which normally restricts cell size to 100 km. The presented work is a clear evidence of the capabilities multi-cell LTE offers for over-sea communication services. However, firstly the measurement campaign was performed using a ship, which implies significantly lower mobile speed than what has to be expected by providing UAVs and secondly, the throughput of both base stations were measured independently and were not combined to one data stream, as it will be in this work.

II. Methodology and System Model

In order to show the benefit of multilink aggregation a hardware-in-the-loop experiment is conducted. Making use of a channel emulator as well as software-defined radio LTE base station and industrial grade modems the extensive runs serves as a pre field trial study. The following section introduces the main concepts of the maritime model and multilink aggregation protocol MPTCP.

A. Case Study: UAV during Search and Rescue Mission

The methodology and methods presented below are applied to the scenario where one UAV conducts a SAR mission. The UAV is launched close to the coast and withdraws from the ground station with a continuous speed. To increase both reliability and data rate on the communication link, the vehicle is equipped with two LTE modems (UEs). Each modem is assigned to an individual Mobile Network Operator (MNO), operating on individual frequencies (frequency diversity). The base stations are assumed to be located on-shore and next to the starting location of the UAV close to the coast. Site-diversity as well as flight trajectory planning is not considered as part of this work. The first LTE link is operated by public MNO on a low frequency. The second link is a dedicated Long Range LTE link using different, higher frequency. In addition, tracking antennas are considered. Both links are combined on the transportation layer using MPTCP. MPTCP appears transparent to the application layer and allows seamless hand-overs between different communication links. The scenario is fully summarized in Fig. 1.

B. Maritime Channel Modeling

In order to realistically represent the maritime scenario the radio channel propagation extends the empirical model for A2G communication [11]. This model has been derived by a measurement campaign performed in cooperation with the National Aeronautics and Space Administration (NASA). The underlying model has been implemented as a tapped delay line (TDL) model. The channel impulse response h_f for a specific frequency band f follows the equation of a Curved-Earth Two-Ray (CE2R) model:

$$\begin{aligned} h_f(\tau) = \alpha_0 \; e^{-j2\pi R_1/\lambda} \; \delta(\tau - \tau_0) \\ + \alpha_s \; e^{-j2\pi R_2/\lambda} \; \delta(\tau - \tau_s) \; \Gamma_F \; D_k \; r_f \end{aligned} \tag{1}$$

The first summand characterizes the Line-of-Sight portion of signal attenuation, with R_1 being the direct distance between UAV and ground station. The second summand provides the Multipath propagation of the sea surface reflected path with length R_2. The amplitude coefficients of both paths are defined as $\alpha_i = c/(4\pi f R_i)$. A little more in detail, the specific surface reflection coefficient $\Gamma_{k,f}$ depends on frequency, grazing angle and the environment. To imitate maritime environment the tabulated sea saltwater model from 2.3.1 in [12] has been applied to quantify Γ_f. The calculation of the divergence factor D depends on the length of the surface reflection path as well as the grazing angle Ψ. [11] provides an easy-to-implement algorithm to calculate these purely geometric values.

In maritime scenarios, speed of wind has a major impact on the surface roughness r_f. Higher wind speeds are considered to lead to higher sea states, which in turn causes the reflected wave to scatter at the sea surface. The evaluation of the surface roughness models provided in [12] and [13] results in the surface coefficient C_r:

$$C_r = 4\pi \; 0.0051 u^2 \; sin(\Psi)/\lambda \tag{2}$$

Herein, u describes the wind speed in Meters per second, Ψ the grazing angle of the wave and λ the wavelength. According to the Miller-Brown model [14] surface reflection can be calculated using the first order modified Bessel function I_0:

$$r_f = exp(-C_r^2/2) I_0(-C_r^2/2) \tag{3}$$

The authors of [11] further suggest to model the remaining bundled diffuse multipath propagation in an additional third tap, which is stochastically modeled in both occurrence and duration ones appeared. Due to the fact, that the influence of this tap was found to be marginal and only present with a very low probability for link distances over $5\ km$, the third tap will be neglected within the scope of this work to further ensure reproducibility and transparency of the results. Both remaining taps are deterministic and represented in amplitude, phase shift and delay.

C. LTE Timing Advance Emulation

The second enhancement refers to timing synchronization of all mobile participants of the network, user equipments (sUEs), and the Base Station (BS), which is crucial to support large cell sizes in LTE. To ensure temporal alignment and

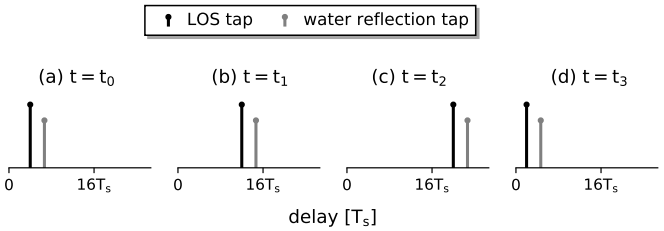

Fig. 2. Qualitative illustration of the proposed uplink TA emulation. The shown time-series represents rising distances between UAV and BS from (a) to (d). In (c), the relative path delay of the first tap exceeds the TA quantization step, which triggers a virtual increment of the TA parameter, which in turn shifts both taps ahead by 16 T_s.

TABLE I. PARAMETRIZATION OF EXPERIMENTAL EVALUATION

BS label	UAV tx power	UAV gain	carrier frequency	BS gain	BS sens.	BS height
BS1	20 dBm	3 dBi	800 MHz	8 dBi	−102 dBm	100 m
BS2	20 dBm	3 dBi	2.6 GHz	24 dBi	−95 dBm	20 m

thus collision-free transmissions and receptions of subframes, the UE's transmissions are shifted ahead in time depending on their individual distances to the BS. This time shift is measured in the downlink and applied to the uplink in quantization steps of 16 T_s, where $T_s \approx 30.26\ ns$ is the basic timing unit. Considering the propagation speed of electromagnetic waves, each quantization step corresponds to intervals of $78.12\ m$ Line of Sight (LOS) distance. Due to the fact, that the used LTE equipment in this work is not able to fully support this standardized TA mechanism, another solution was found by integrating the resulting time shifts into the uplink channel model, assuming a functional TA. The proposed approach is illustrated in Fig. 2. Under the line, the proposed algorithm models the path delays occurring at the receiver of the BS similar to what would be observable at a real system.

D. Antenna Modeling

The last channel model enhancement contains the integration of path-sensitive BS antenna gains, which in this work are oriented at real antennas. The vertical antenna pattern of each a parabolic dish antenna with 24 dBi gain, a full width at half maximum (FWHM) of 6° and an operating frequency of 2.4 GHz as well as a patch antenna with 8 dBi gain, a FWHM of 32° and an operating frequency of 800 MHz were modeled as mathematical approximations. Subsequently, a path-specific gain using these models is applied to both propagation paths. Here, an accurate antenna tracking conceivably enabled through UAV GPS data is assumed, leading to full antenna gains for the LOS path and angle of incidence dependent gains for the indirect path. The proposed antenna modeling of path specific gains leads to much more realistic representations of interference patterns, especially in distances close to the BS. This can be explained by the large angle of incidence of the second path in this regions, whereas the angle decreases with a rising distance.

E. Evaluation Setup

Before the results of the laboratory experiments are discussed, the methodology for the proposed close-to-reality hardware-in-the-loop simulation setup is presented. An illustration of the procedure can be seen in Fig. 3. The setup consists of two *tinyLTE* [15] base stations, which are connected with wires via the channel matrix to two industrial grade *Sierra Wireless MC7455* LTE modems. The channel matrix applies the previously introduced maritime channel model in form of a signal attenuation.

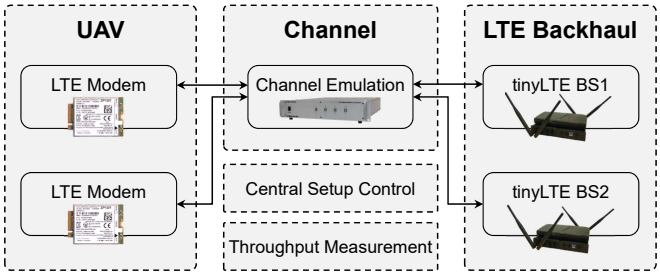

Fig. 3. Hardware in the Loop (HIL) experiment makes use of two separate commercial of the shelf LTE modems. Channel matrix applies the maritime channel model. Two LTE base stations are setup using tinyLTE.

The Hardware-in-the-Loop (HIL) experiment starts with the previously described generation of channel impulse responses in the maritime environment, based on the positioning of the BSs, the UAV trajectory and other environmental influences. As the input power level of the channel emulator is limited, the taps of the maritime channel model were normalized. After the superposition of the individual taps, an estimate of the received signal power S_{dBm} is created. The channel matrix applies target attenuation until target Signal to Noise Ratio (SNR) is achieved by $SNR = S - N - F$. Typical noise floor N and the device's individual noise figure F are provided in table I.

The parametrization of the experiment is chosen to represent both a typical BS as experienced in public LTE networks as well as a dedicated BS according to [16]. The complete parametrization can be found in Tab. I.

F. MPTCP-based Link Aggregation

The multilink aggregation makes use of the transport layer protocol MPTCP. For the evaluation MPTCP-enabled Linux kernels in version 4.14.105 were installed both in UAV as well as ground station. MPTCP supports two major schedulers. The default scheduler *maximizes throughput*, by scheduling data on both data links, prioritizing the link with the lowest round-trip time. The *redundant* scheduler sends identical data over every available link. In case of packet loss or varying round-trip times, the latency of data delivery is minimized at the cost of a lower application layer throughput. Latter one is the proposed scheduler for telemetry and control data or low bitrate real-time video streams, as the former one may be utilized for high volume payloads.

III. SYSTEM EVALUATION

The introduced system model and maritime A2G channel is finalized by the evaluation of the expected UAV link reliability with respect to the distance, both for heterogeneous single

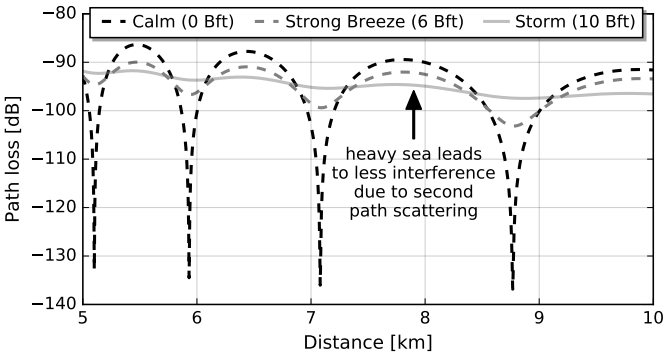

Fig. 4. Influence of wind speed on the path loss of the proposed maritime Air-to-Ground (A2G) channel model. Distance is measured as ground distance between ground station and UAV. Note the weakened interference pattern occurring at higher wind speeds, due to second path scattering at the rougher sea surface.

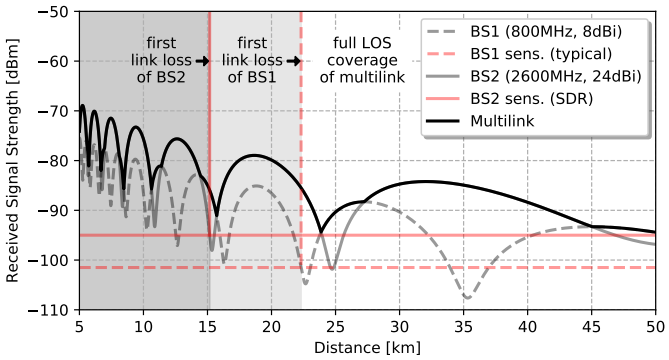

Fig. 5. Example of received signal strength over distance comparison between public (BS1) and dedicated LTE (BS2). As soon as the received signal strength drops below receiver sensitivity connectivity is assumed to be lost and UAV returns to its starting position marking the maximum achievable distance in SAR missions. The Multilink approach enables connectivity over the full Line-of-Sight (LOS) distance.

links as well as the combined multilink, which can be seen as a link diversity approach on RF-level. Research object is the influence of the UAV flight level on the one hand and the wind speed (not the flight speed) on the other hand, each affecting radio signal propagation. Furthermore, the analysis is executed for two heterogeneous basestations in terms of individual receiver sensitivities and antenna patterns.

A. *Impact of Wind Speed on A2G Link*

In order to evaluate the impact of wind speed on the A2G link an analytic evaluation of the channel model is performed. Fig. 4 illustrates the path loss in dependency of the UAV to BS distance and wind speed. With calm wind speed (0 Bft) the model approximates to a two-ray path loss pattern as the radio signal is reflected on the smooth sea surface. With higher wind speeds the sea becomes rougher, thus resulting in weaker interference patterns at the receiver as the indirect path is less dominant. In the storm scenario (10 Bft) nearly no secondary path interferences occur. On the one hand, from channel modeling perspective this is beneficial. However, on the other hand in this scenario wind speeds of approx. 100 km/h cause major challenges for the UAV flight operation.

B. *Communication Range Analysis*

In a next step, the availability and thereby the reliability of communication links is investigated. For safety reasons, the autopilot of the UAV is supposed to return to its home location when connectivity to the ground station is lost. Therefore, a hard criteria for the estimation of stable link distances has been defined: communication link between UAV and BS is defined as disconnected (or unavailable), if either the received signal strength drops under the respective receiver sensitivity or the maximum LOS distance defined by the CE2R part of the channel model is reached. For the multilink approach, both single links need to be unavailable for rating a distance as unstable. Fig. 5 illustrates the received signal strength over distance between UAV and base station. As soon as the received signal strength drops below the receiver sensitivity connection is lost and the UAV is supposed to return to its home location. Depending on the wind speed signal second path interferences

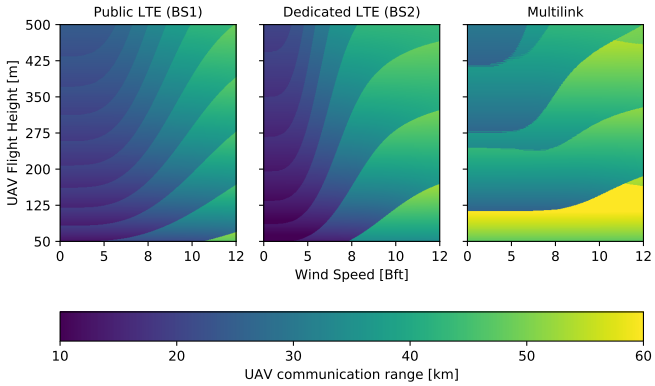

Fig. 6. Analytic estimate of the achievable communication ranges for both individual MNO as well as combined Multilink system. The UAV communication range represents the distance when communication link is interrupted either by dropping below receiver sensitivity or due to loss of the Line of Sight (LOS).

cause major signal losses over several kilometers, e.g. BS1 signal between 34 km and 36 km.

C. *Multilink Communication Range Improvements*

Figure 6 presents the resulting analytical maximum UAV link distances in the form of a heat map in dependency of wind speed and flight height. The first aspect to be noticed is that, for both single link evaluations, a qualitatively similar pattern with hard steps is observable. These steps can be explained by the combination of the aforementioned hard condition and the channel model characteristics with the strong two-ray interferences (c.f. Fig. 5). A small displacement of these destructive interferences, which may be caused by variation of wind speed or UAV flight altitude, decides between the received power dropping below receiver sensitivity or not. One major point that can be underlined here is the expected overall superiority of the multilink over both single links. As the interference patterns of a single link can be compensated by the other link, multilink communication range is much higher. Qualitatively similar, but much less distinct patterns can be

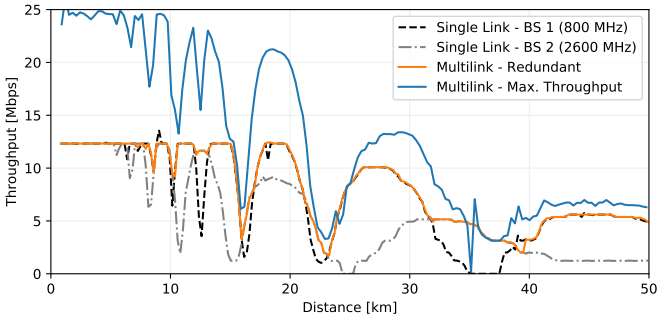

Fig. 7. Result of Hardware-in-the-Loop (HIL) experiment of UAV flying at 100 m altitude at 5 Bft wind speed. Multilink aggregation compensates drops in data rate of single links.

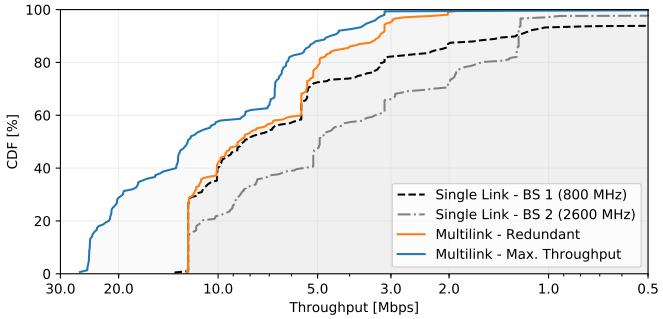

Fig. 8. Empirical cumulative distribution function (CDF) of the previous throughput experiment shows MPTCP's increased application layer data rate.

found. This is due to the fact, that the different interference patterns of the two individual links complement each other on a physical level resulting in higher robustness of the multilink. Given the chosen parametrization, this effect is significant at an altitude of roughly 100 m, where reliable UAV link distances are only restricted by earth's curvature and thus mainly unaffected by wind speed. Since the wind speed cannot be influenced during SAR missions, a flight altitude of approx. 100 m is recommended, without considering any aspects other than the communication characteristics.

D. Experimental Throughput Evaluation

The following section provides the throughput evaluation of the HIL experiment. The experiment was conducted for both single links and afterward using MPTCP link aggregation in *default* and in *redundant* mode. The first one utilizes both links in order to maximize the throughput. The latter sends data redundantly over all available links and hereby minimizes application layer latency. Fig. 7 shows the throughput in dependency of the overground distance for a UAV with 100 m altitude and 5 Bft wind speed. The second path interferences are clearly visible in variations of the resulting application layer throughput. Both LTE networks show a lot of drops in the data rate. MPTCP in *redundant* mode achieves as much throughput as the best single link. In *maximum throughput* mode, multilink throughput is the sum of both single links. However, if in the default mode packet loss occurs, packets need to be retransmitted increasing the application layer latency. This effect can be seen at a distance of 35 km, where the connectivity of BS 1 drops and in-flight data of this link is lost. Therefore, these packets need to be retransmitted. As MPTCP supports selective acknowledgments this results in a slight overshoot in application layer data rate right after lost packets have been retransmitted.

E. MPTCP enabled data rate improvements

In the next step, the benefit of MPTCP enabled multilink aggregation will be statistically verified. Fig. 8 shows the empirical cumulative distribution function (CDF) of the throughput of the previous experiment. For illustration purposes, the throughput axis has been plotted logarithmically.

Even though both single links provide a decent average throughput they are unable to offer connectivity over the whole distance of 50 km. Due to interference-based loss of connection the first link (BS 1) achieves only 93 % availability, whereas BS 2 is available 97 % of the distance.

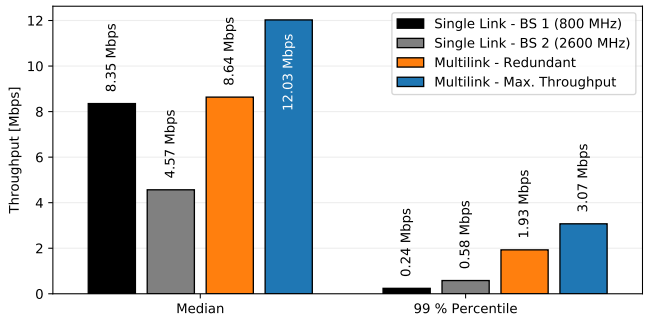

Fig. 9. Overall HIL experiment results: mean and minimum throughputs (99 % percentiles) of a UAV with flight height 100 m for varying wind speeds (0 – 11 Bft). MPTCP link aggregation shows significant boost in air-to-ground data rate.

Aggregation of the multiple links in *redundant* mode provides a minimum data rate of at least 1.93 $Mbps$ and *max. throughput* mode results in a minimum of 3.07 $Mbps$. Hereby, MPTCP complements both communication links: the first link (BS 1) benefits from an increased availability; the second link's (BS 2) average throughput is significantly increased.

The same effect is reflected in the overall evaluation, which is presented in Fig. 9. The figure shows the average data rate as well as minimum throughput in form of the 99 % percentiles of a UAV with a flight altitude of 100 m, a speed of 100 km/h and changing wind speeds between 0 Bft and 12 Bft. In terms of mean throughput especially the BS 2 benefits from a two to threefold improvement by MPTCP. The first single link increases by 3.5 $Mbps$ on average in MPTCP max. throughput node. The minimum throughput improves significantly for both single links when MPTCP is leveraged, because of the increased connectivity. All in all MPTCP multilink aggregation is highly beneficial for maritime SAR missions.

F. Trade-off between Throughput and Latency

As previously described MPTCP supports two schedulers. Whereas the default scheduler maximizes the throughput, the redundant scheduler improves robustness and communication latency. Hereby the scheduler transmits a copy of a transmittable data and sends these copies over each path simultaneously. The receiver is able to reassemble the transmitted data

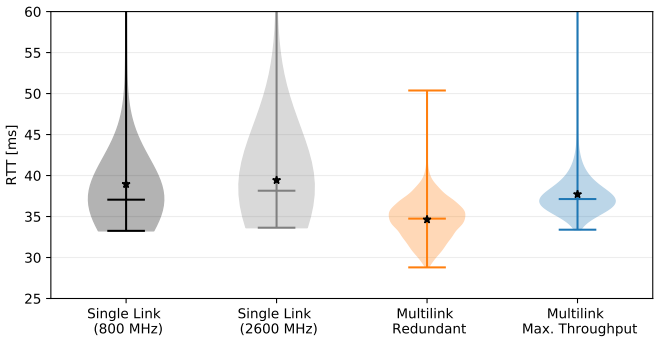

Fig. 10. Experimental latency evaluation of the UAV link during flight with wind speed of 5 Bft. Redundant MPTCP scheduling results in lower mean and maximum Round Trip Time (RTT) than single link or maximum throughput MPTCP scheduler.

based on the earliest received packet. In case of packet loss, e.g. occurring when connectivity of one link drops, data will be received via the second path. The max. throughput scheduler would require a retransmission via the remaining path leading to an increased latency. To assess and evaluate the redundant scheduler a constant bitrate stream of approx. 160 $kbps$ was sent from the UAV to the ground station, imitating a telemetry data link. Fig. 10 shows the resulting Round Trip Time (RTT) evaluation for the same flight as the previous throughput evaluation (5 Bft wind speed, 100 km/h UAV speed). The redundant scheduler the lowest average latency. In addition, its whole distribution, as indicated by the violin plot, lies significantly below the other experiment runs. Outliers of the single link experiments range up to 2000 ms as a result of the link outages. During link outages no new packages were scheduled - otherwise the distributions would result in a much higher latency. The maximum throughput scheduler performs as it distributes data on all paths. When one link of the multiple links breaks up, packet loss occurs. Retransmissions via the secondary path lead to a higher latency.

IV. Conclusion and Future Work

Within the scope of this work MPTCP-enabled link aggregation for maritime search and rescue missions is evaluated. In a first step, a detailed and realistic maritime air-to-ground channel model is derived. Analytic evaluation of the channel model promise an improvement of coverage as well as throughput by combining heterogeneous links. In a second step, the model is evaluated in a hardware-in-the simulation loop. Empirical results highlight the improvements both in communication range and data rate of the default MPTCP scheduler, which aims at maximizing throughput. On the other hand, the redundant multilink scheduler optimizes for lowest latency communication and is therefore recommended for telemetry and control data. For future work, the evaluation of the channel model in field tests, using the very same hardware from the empiric evaluation, is pursued.

Acknowledgment

The work on this paper has been partially funded by the German Federal Ministry of Education and Research (BMBF) for the projects LARUS (Supporting Maritime Search and Rescue Missions with Unmanned Aircraft Systems, 13N14133) and A-DRZ (Establishment of the German Rescue Robotics Center, 13N14857) as well as the Deutsche Forschungsgemeinschaft (DFG) within the Collaborative Research Center SFB 876 "Providing Information by Resource-Constrained Analysis", project B4.

References

[1] A. C. Watts, V. G. Ambrosia, and E. A. Hinkley, "Unmanned Aircraft Systems in Remote Sensing and Scientific Research: Classification and Considerations of Use," *Remote Sensing*, vol. 4, no. 6, pp. 1671–1692, 2012.

[2] LARUS research project website. [Online]. Available: https://larus.kn.e-technik.tu-dortmund.de/

[3] 3GPP, "Feasibility Study on Maritime Communication Services over 3GPP system," 3rd Generation Partnership Project (3GPP), Technical Report (TR) 22.819, 06 2018, version 16.0.0. [Online]. Available: https://portal.3gpp.org/desktopmodules/Specifications/SpecificationDetails.aspx?specificationId=3134

[4] W.-S. Jung, J. Yim, and Y.-B. Ko, "Ultra long range LTE ocean coverage solution," in *2017 24th International Conference on Telecommunications (ICT)*, May 2017, pp. 1–5.

[5] C. Raiciu, C. Paasch, S. Barre, A. Ford, M. Honda, F. Duchene, O. Bonaventure, and M. Handley, "How hard can it be? designing and implementing a deployable multipath TCP," in *9th USENIX Symposium on Networked Systems Design and Implementation (NSDI 12)*. San Jose, CA: USENIX Association, 2012, pp. 399–412. [Online]. Available: https://www.usenix.org/conference/nsdi12/technical-sessions/presentation/raiciu

[6] Q. De Coninck and O. Bonaventure, "Multipath QUIC: Design and Evaluation," in *Proceedings of the 13th International Conference on emerging Networking EXperiments and Technologies*. ACM, 2017, pp. 160–166.

[7] D. Behnke, M. Priebe, S. Rohde, K. Heimann, and C. Wietfeld, "ScalaNC - Scalable heterogeneous link aggregation enabled by Network Coding," in *13th IEEE International Conference on Wireless and Mobile Computing, Networking and Communications (WiMob 2017) - Fourth International Workshop on Emergency Networks for Public Protection and Disaster Relief (EN4PPDR'17)*, oct 2017.

[8] W.-S. Jung, J. Yim, and Y.-B. Ko, "Adaptive offloading with MPTCP for unmanned aerial vehicle surveillance system," *Annals of Telecommunications*, vol. 73, no. 9, pp. 613–626, Oct 2018. [Online]. Available: https://doi.org/10.1007/s12243-018-0660-5

[9] R. M. N. Chirwa and A. P. Lauf, "Performance improvement of transmission in unmanned aerial systems using multipath TCP," in *2014 IEEE International Symposium on Signal Processing and Information Technology (ISSPIT)*, Dec 2014, pp. 000 019–000 024.

[10] M. Park, H. Seo, P. Park, Y. Kim, and J. Jeong, "LTE maritime coverage solution and ocean propagation loss model," in *2017 International Conference on Performance Evaluation and Modeling in Wired and Wireless Networks (PEMWN)*, Nov 2017, pp. 1–5.

[11] D. W. Matolak and R. Sun, "Air–Ground Channel Characterization for Unmanned Aircraft Systems—Part I: Methods, Measurements, and Models for Over-Water Settings," *IEEE Transactions on Vehicular Technology*, vol. 66, no. 1, pp. 26–44, Jan 2017.

[12] J. D. Parsons, *The mobile radio propagation channel*. Wiley Online Library, 2000.

[13] R. Vaughan and J. B. Andersen, *Channels, propagation and antennas for mobile communications*. Iet, 2003, vol. 50.

[14] A. Miller, R. Brown, and E. Vegh, "New derivation for the rough-surface reflection coefficient and for the distribution of sea-wave elevations," *Microwaves, Optics and Antennas, IEE Proceedings H*, vol. 131, pp. 114 – 116, 05 1984.

[15] F. Eckermann, P. Gorczak, and C. Wietfeld, "tinylte: Lightweight, ad hoc deployable cellular network for vehicular communication," in *IEEE Vehicular Technology Conference (VTC-Spring)*, Jun 2018. [Online]. Available: https://arxiv.org/abs/1802.09262

[16] 3GPP, "Evolved Universal Terrestrial Radio Access (E-UTRA); Base Station (BS) radio transmission and reception," 3rd Generation Partnership Project (3GPP), Technical Specification (TS) 36.104, 07 2018, version 14.8.0.